PROCEEDINGS of the
23rd International Congress on Acoustics

9 to 13 September 2019 in Aachen, Germany

Numerical and experimental investigation of the turbofan first booster stage tone noise

Victor Mileshin, Sergey Pankov, Anton Rossikhin[1]

Central Institute of Aviation Motors, Russia

ABSTRACT

An important problem of turbofan design is maintenance of low noise emission. One of the components of turbofan noise is the tone noise arising due to inter-row interactions in the booster stages. For modern turbofans this component of noise can be significant at approach certification point. The investigations of the tone noise of the first booster stage have been carried out in CIAM during last several years. They were performed using a frequency domain method for simulation of tone noise of multistage turbomachines developed in CIAM. The advantage of the method is the high speed of calculations; however it relies on some ad hoc assumptions about the process of interactions between flow field disturbances and blade rows. This work presents the results of the tone noise calculation of the first booster stage using time domain approach based on multirate Runge-Kutta scheme. The result, obtained in the calculation, is independent from any assumptions about the interactions in the multistage turbomachine. This allows verifying the results of previous calculations. In general satisfactory correspondence were found between the results of computations in time and in frequency domains and between them and experimental data obtained in the CIAM C-3A acoustic test facility.

Keywords: tone noise, booster stages, multirate Runge-Kutta scheme

1. INTRODUCTION

The main source of modern turbofan noise is the fan. However, such sources of tone noise, as low pressure turbines and boosters, can also contribute to the tone noise at some operational conditions [1,2]. The advances in the reduction of a fan tone noise can make the contribution of these sources more significant. The increase of the low pressure cascades shaft rotation speed in the modern turbofans can also lead to the same result. The feature of low pressure turbines and boosters is that they are usually multistage turbomachines. The necessity of taking into account of interactions between different stages significantly complicates simulations of their tone noise [2,3,4] in comparison with ordinary fans.

A method of multistage turbomachines tone noise calculation, formulated in the frequency domain, was developed in CIAM as a part of activities devoted to the calculation of tone noise of the booster stages. It is based on the kinematic relations, describing a dependence of flow field in a turbomachine from time and azimuth angle. The flow field in each row is represented according to the method as a combination of harmonic fragments in one blade channel. The notion of harmonic fragment – an assembly of disturbances having equal frequency and phase shift between the boundaries of one blade channel was introduced in [5] (see also references therein). As it was shown in the paper [5], a flow field in a row can be decomposed into fields of harmonics of some base frequency, and each field of harmonic can be decomposed into a finite number of fields of harmonic fragments. The number depends on the turbomachine geometry only. For example for single stage turboimachine the flow field for each harmonic can be described by only one harmonic fragment, which reduces the method introduced in [5] to the well-known method of rotor-stator interaction calculation based on phase-lagged boundary conditions [6]. The method, developed in CIAM, makes possible a significant reduction of computational resources, needed for a turbomachine tone noise simulation, by taking into account only those harmonic fragments, which contain the strongest disturbances, generated by the turbomachine.

However the specification of the set of harmonic fragments, needed for the calculation of a

[1] aarossikhin@ciam.ru

turnomachine tone noise with sufficient prediction, is impossible without some heuristic considerations [5]. Though the results of the calculations with the method, showed satisfactory correspondence with experimental data, it seems important to compare these results with those obtained by a method of calculation being less sensitive to the assumptions, made at the statement of the calculations.

Such method of calculation is the method of calculation in the time domain. According to this method the discretized equations are solved for specified number of time steps. The calculation is performed for whole spatial period (a sector of full annulus equal to $2\pi/P$, where P is the greatest common divisor of numbers of blades in blade rows). In such a calculation all disturbances, generated by turbomachine, which can be resolved on the computational grid with the specified time step are taken into account. Unfortunately the method is extremely expensive in terms of computational resources.

The paper is devoted to the application of the time domain method of calculation for the problem of the first booster stage tone noise, which was earlier considered in [5] with the usage of the frequency domain method. Both methods of calculation are implemented in CIAM 3DAS solver [7,8]. The solver was designed for the calculation of tone noise of the conventional and counter-rotating fans, open rotors, low pressure turbines and compressors.

2. 3DAS SOLVER

2.1 The Description of the Solver

The method of calculation used in the 3DAS solver is based on the decomposition of the unsteady viscous flow into two parts - inhomogeneous viscous steady flow field and unsteady inviscid disturbances. For turbomachinery tone noise applications the steady mean flow field in rows can be calculated by any steady aerodynamic solver using Reynolds-Averaged Navier–Stokes (RANS) equations, structured grid, finite volume spatial approximation and "mixing-plane" interfaces between rows. Calculation of unsteady inviscid equations for disturbances (linear or nonlinear dependent on the problem) over the mean steady flow field in a row in the reference frame, rotating with the row, is performed by 3DAS solver.

The equations are solved using the numerical methods of computational aeroacoustics. The finite volume approach is used for spatial discretization. The fluxes are approximated using fourth order DRP (Dispersion Relation Preserving) scheme [9]. The details of the DRP scheme implementation can be found in [7] and references therein.

Different Runge-Kutta schemes or dual time step method can be used in 3DAS solver as advancing schemes. Usually second-order four stages Runge-Kutta LDDRK (Low Dissipation and Dispersion Runge-Kutta Scheme) scheme [10] was used for calculations in the time domain. Also a multirate Runge-Kutta scheme, developed by authors on the bases of LDDRK scheme can be applied when the computational domain can be divided on several subdomains with significantly different cell sizes.

3DAS solver can be used for calculations either in the time domain or in the frequency domain. In the first case the direct evaluation of the discretized equations solution for the prespecified number of steps is performed. The interaction between blade rows is provided using sliding grid interfaces. In the second case the solution is searched in the form of a finite set of fields of harmonic fragments, sufficient for the description of flow field evolution in time. It is obtained using the pseudotime relaxation method with local time step. The interaction between blade rows is provided by special interfaces, which preserve continuity of flow parameters for prespecified set of harmonic functions of time and circumferential angle (circumferential modes).

Other important details about 3DAS solver can be found in [8].

2.2 Multirate Runge-Kutta Scheme

The second-order four stages Runge-Kutta LDDRK scheme is the usual choice for calculations in the time domain with 3DAS solver. The examples of calculations with the scheme can be found in [11] and references therein. However the explicit scheme can be used only on the grids with relatively large minimal cell sizes. The situation is different for frequency domain methods, where there are no limitations on the cell sizes. The problem under consideration was first formulated in the frequency domain, and it was found out that the calculation on the same grid in the time domain using explicit scheme demanded too much time steps on one period of rotation. As alternatives two methods of calculations were tested – dual time step method and multirate Runge-Kutta scheme. The latter

approach showed significantly higher calculation speed.

Multirate Runge-Kutta schemes are an attractive approach for the solution of ordinary and partial differential equations. In the formulation of our multirate Runge-Kutta method we followed the approach for construction of such methods presented in [12]. The paper [12] is in turn based on the well-established theory of partitioned Runge-Kutta methods [13].

Let's briefly describe the method. Assume that we have a system of ordinary differential equations:

$$\dot{y}(t) = f(t, y),\ y \in R^n,\ y(t_0) = y_0,\ t > t_0 \tag{1}$$

In the following we will assume that the solution of equation (1) can be split into two components $y_L(t)$ and $y_A(t)$, where the first of the components (latent) varies relatively small in time in comparison with the second component (active). For the components we can write out:

$$\dot{y}_A(t) = f_A(y_A, y_L),\ \dot{y}_L(t) = f_L(y_A, y_L),\ y_A \in R^{n_A},\ y_L \in R^{n_L}, n_A + n_L = n \tag{2}$$

The latent component can be integrated with the time step H, while active with the time step $h=H/p$ (p – integer). Thus following the standard representation of the Runge-Kutta scheme we can express the solution for the latent and the active components in the form

$$\begin{aligned} &k^{\lambda}_{A,i} = f_A(y_{A,\lambda} + h\textstyle\sum_{j=1}^{s} a_{ij} k^{\lambda}_{A,j}, \tilde{Y}^{\lambda}_{L,i}),\quad i = 1,2,\ldots,s, \\ &y_{A,\lambda+1} = y_{A,\lambda} + h\textstyle\sum_{i=1}^{s} b_i k^{\lambda}_{A,i} \approx y_A(t_0 + (\lambda+1)h), \\ &\lambda = 0,1,2,\ldots,p-1,\quad \tilde{Y}^{\lambda}_{L,i} \approx y_L(t_0 + (\lambda + c_i)h). \end{aligned} \tag{3}$$

$$\begin{aligned} &k_{L,i} = f_L(\tilde{Y}_{A,i}, y_{L,0} + H\textstyle\sum_{j=1}^{\bar{s}} \bar{a}_{ij} k_{L,j}),\quad i = 1,2,\ldots,\bar{s}, \\ &y_{L,1} = y_{L,0} + H\textstyle\sum_{i=1}^{\bar{s}} \bar{b}_i k_{L,i} \approx y_L(t_0 + H),\quad \tilde{Y}_{A,i} \approx y_A(t_0 + \bar{c}_i h) \end{aligned} \tag{4}$$

Here $c_i = \sum_{j=1}^{s} a_{ij}$, a $\bar{c}_i = \sum_{j=1}^{\bar{s}} \bar{a}_{ij}$.

The main question in the problem of construction of multirate advancing scheme is how to find the contribution of passive components in the time evolution of active and vice versa. Following [12] we are using interpolation formulas of the form

$$\begin{aligned} &\tilde{Y}^{\lambda}_{L,i} = y_{L,0} + h\textstyle\sum_{j=1}^{\bar{s}} (\gamma_{ij} + \eta_j(\lambda)) k_{Lj},\quad i = 1,2,\ldots,s,\quad \lambda = 0,1,\ldots p-1, \\ &Y_{A,i} = y_{A,0} + H\textstyle\sum_{j=1}^{s} \bar{\gamma}_{ij} k^0_{A,j},\quad i = 1,2,\ldots,\bar{s} \end{aligned} \tag{5}$$

The constants in the formulas (5) should obey special assumptions in order to provide the desired order of the scheme. Using the theory of partitioned Runge-Kutta methods it is possible to show, that in order to preserve the second order the constants should satisfy the following conditions [12]:

$$\textstyle\sum_{j=1}^{\bar{s}} \eta_j(\lambda) = \lambda,\quad \sum_{j=1}^{\bar{s}} \gamma_{ij} = c_i,\quad i = 1,2,\ldots,s,\quad \sum_{j=1}^{s} \bar{\gamma}_{ij} = \bar{c}_i,\quad i = 1,2,\ldots,\bar{s}, \tag{6}$$

In this paper we will use the previously mentioned second order LDDRK scheme as a base for the construction of multirate scheme. The constants for the LDDRK scheme are:

$s=4;\ b_1 = b_2 = b_3 = 0;\ b_4 = 1.0;\ a_{2,1} = 0.234570947137;\ a_{3,1} = 0;\ a_{3,2} = 0.333333333333333;$

$$a_{4,1} = a_{4,2} = 0;\ a_{4,3} = 0.5.$$

The constants in our multirate scheme are the same for both active and latent components. As for the formulas (5) we assumed that the values for $\gamma_{i,j}$ are the same as for $a_{i,j}$ (again both for active and latent components):

$$\gamma_{2,1} = 0.234570947137;\ \gamma_{3,1} = 0;\ \gamma_{3,2} = 0.333333333333333;\ \gamma_{4,1} = \gamma_{4,2} = 0;\ \gamma_{4,3} = 0.5,$$

Also it was assumed that $\eta_1 = \eta_2 = \eta_3 = 0;\ \eta_4 = \lambda$. This choice of the constants satisfies conditions (6).

If we have several levels of variables activity we have to introduce several time scales. For the level of activity l, $l=0..k$, it is reasonable to take time step in the form $h_l=H/p^l$ so that to preserve the integer ratio between time steps corresponding to different levels of activity. In our calculations it is usually assumed that $p=2$.

The scheme under consideration can provide relatively high computational speed. However it has some significant disadvantages. First of all it is not conservative, being applied to partial differential

equations. Also in some cases there is a lack of stability.

3. THE OBJECT OF INVESTIGATION

The fan under consideration is a 700 mm diameter high bypass ratio wide chord fan model with swept stator vanes, designed for an advanced turbofan of civil aircraft. It has three booster stages. The description of the model can be found in [5] and in references therein.

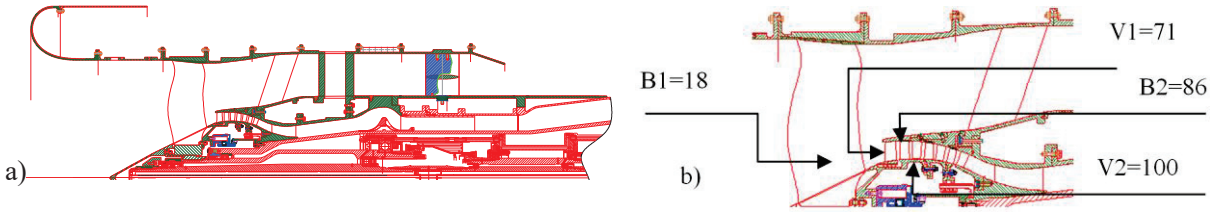

Figure 1. - Scheme of the fan model: a) general view; b) magnified fragment

The model has 18 blades in the fan rotor and 41 vanes in the stator of bypass duct. It also has 71 vanes in the inlet guide vanes (IGV) of the booster stages, 86 blades in the rotor of the first booster stage and 100 blades in the stator of the first stages. The scheme of a fan model can be seen in the fig. 1.

The calculation was performed at approach operational conditions. At these conditions the tone noise of the booster stages dominates in the forward hemisphere over the tone noise of the fan rotor-stator interaction [14]. Design parameters of the fan model at approach and designed mode are represented in Table 1.

Table 1. Parameters of the fan model

	Design	Approach
Relative shaft speed	100%	53.9%
Fan rotor tip speed	395 m/s	212.9 m/s
First stage rotor tip speed	221.5 m/s	119.4 m/s
Bypass ratio	8.5	9.7

The aim of the calculation is to resolve the main tones connected with the first booster stage of the fan model. The noise generation in the first booster stage reveals itself by the tones with frequencies being the combinations of the blade passing frequency of the first booster stage rotor f_2=86N, where N is the shaft rotational frequency and some harmonic of the fan rotor blade passing frequency f_1=18N. The experience obtained in the previous calculation showed [5,15] that the tones arise as a result of the scattering of the disturbance with the frequency equal to f_2 on the fan rotor. Therefore, first of all, there was a task in view to correctly describe mechanisms of the generation of the tone with this frequency in the booster stage. Also it was assumed beneficial to the calculation precision to take into account the mechanisms of tones generation at frequencies f_2-f_1 and f_2+f_1. These considerations were used both in the processes of grid generation and computation setup.

The test campaign for the fan in the rig setup was performed in the C-3A test facility [14]. It is designed for acoustic, aerodynamic, and mechanical investigations of counter rotating and conventional fan models.

4. THE CALCULATION OF TONE NOISE

4.1 Calculation of Steady Flow Field and Computation Setup

The first stage of the simulation was the computation of mean steady flow fields using RANS equations, the semi-empirical model of turbulence, and "mixing-plane" interfaces between blade rows. It was performed with CIAM in-house aerodynamic solvers 3D-IMP_MULTI [7]. The computational domain included one blade passage for rotor, stator and each row of booster stages. The boundaries of

the computational domain and boundaries between blocks for individual rows are shown by black curves in the fig. 2. The size of the computational grid was 5.6 million cells. The grid had H-type and was generated by 3D-IMP_MULTI. The results of the computation were compared with experimental data. Satisfactory correspondence for the fan integral characteristics was obtained for all operation range.

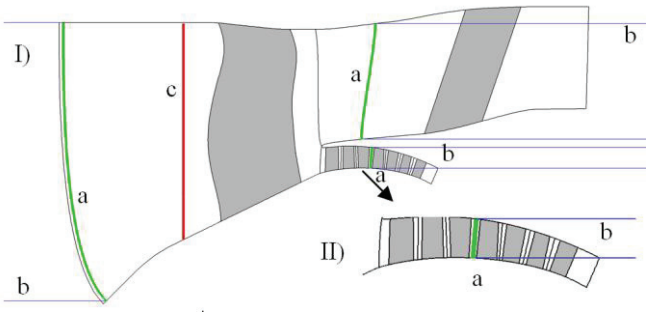

Figure 2. - Scheme of the computational domain: I) Low pressure compressor; II) Booster. Here: a - the boundaries of the fine grid region in the computational domain; b - the boundaries of buffer blocks (shown only partially); c - the surface for modal analysis upstream of the fan

Next step was the generation of the grid for unsteady calculations. Corresponding computational domain included the domain, containing fan rotor blade, the domain containing booster IGV vane, the domains containing rotor and stator blades of the first booster stage and the domain, containing entrance of the bypass duct. We excluded fan stator from the calculation, because our attention was attracted to the forward hemisphere, where booster noise in the experiment was more noticeable. The process of reflection of noise from the stator has been decided to neglect. Also in our calculation we neglected interaction between the noise of the first stage and the second and third stages.

The computational grid for unsteady simulations was derived from the grid for the steady flow field calculations. The grid was resized in X direction in order to provide the propagation of the high-frequency disturbances generated by the first booster stage without significant error. We tried to provide resolution approximately equal to 15 points per wavelength for disturbances which participates in the generation of tones at frequencies f_2-f_1, f_2 and f_2+f_1.

Finally, to avoid unphysical reflections from the boundaries we added to the grid buffer zones in which grid cells are stretched near the outer boundaries. In these blocks outgoing waves are absorbed by numerical viscosity. The boundaries of the fine grid region in the computational domain for unsteady calculations are shown in the fig. 2 by green lines. The boundaries of buffer blocks (partially) are shown in the fig. 2 by the blue lines. The size of the grid was approximately 4.2 million cells.

4.2 Brief Description of the Calculation in the Frequency Domain

Though the article is devoted to the calculation in the time domain, some brief description of the calculation in the frequency domain is needed for a better understanding of the comparison between the results of different computations. The description follows the paper [15], from which we will take the results for comparison (slightly different from those presented in [5] due to higher number of harmonic fragments involved in the calculation).

We started the calculation setup from the determination of those circumferential modes for each of the frequencies of interest (f_1, f_2-f_1 and f_2+f_1), which are cut-on and probably arises in the strongest interactions in the booster stage (the corresponding theory can be found in [5]). It is modes with circumferential numbers m=-43; -14; 15; 28; 44 for f2, modes with m=-32; -3; 10; 26; 39 for f_2-f_1 and modes with m=-38; -25; 4; 33; 46; 62 for f_2+f_1. Most of these circumferential modes arise in the interactions between two or three blade rows. To resolve the modes, in the calculation were involved 67 harmonic fragments: 9 fragments in the first row, 13 fragments in the second row, 23 fragments in the third row and 22 fragments in the fourth row. The size of the problem was equivalent to the one for the calculation in the time domain with 94 million grid cells.

In spite of the large number of variables the calculation converged quite fast. It took approximately 10000 steps for satisfactory and 20000 steps for fine convergence. The results of the calculations will be discussed in the next section.

4.3 Calculation in the Time Domain

The calculation in the time domain was performed in full annulus setup. The computational grid was obtained from the previously described grid for one blade channel. The grid blocks for n-th blade channel were generated by duplication of the blocks in the first blade channel and subsequent turn on to corresponding angle. The size of the final grid was 135 million cells.

The calculation was performed with the usage of multirate Runge-Kutta scheme, described earlier. The number of time steps for one period of rotation was 25250. There were at least 170 steps per period for any of disturbance among those which were resolved in the framework of the frequency domain method. This gave significant reserve in time resolution for the calculation.

It took approximately one and the half periods of rotation for a solution to converge. In fig. 3 are shown the results of calculation as the instantaneous fields of static pressure (pulsations over steady flow field) on the sections of constant diameter d=0.5D, where D is the diameter of the fan. We see quite complex structure of the flow field.

The accumulation of data for modal analyses was started when the solutions had converged (and it took whole period of rotation). The surface, on which modal analysis was performed, is shown in fig. 2 by red curve. The results of the modal analysis in the form of sound power levels of separate circumferential modes are shown in fig. 4. The modes are designated by the pair of integers (h,m), where h is the number of harmonic of shaft rotation frequency and m – circumferential order. The modes which power levels are lower than those of the strongest modes on more than 15 dB are not shown. Also only the modes with frequency less or equal to 122 harmonic of shaft rotation frequency are shown in fig. 4, as the grid had insufficient resolution for the modes with higher frequency.

The results of the calculation in the frequency domain are also plotted in fig. 4. We see that both calculations predict the same set of the strongest modes, and the sound power levels of the modes, obtained in the different calculations are close to each other.

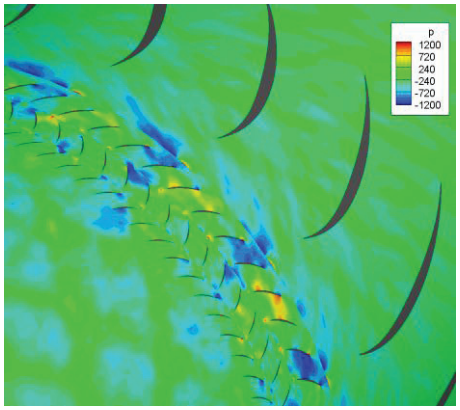

Figure 3. – Unsteady pulsations of static pressure field on the section of constant diameter d=0.5D

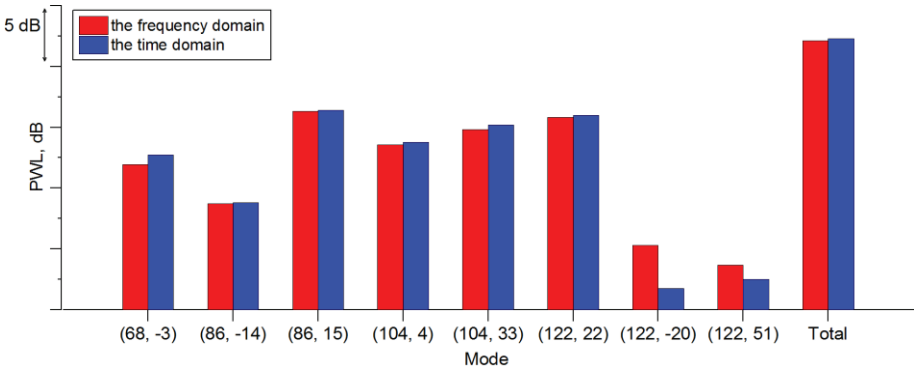

Figure 4. – Results of the modal analysis upstream of the fan. The modes are designated by the pair of integers (h,m).

In general the calculation in the time domain took much more time than the calculation in the

frequency domain. One time step in the frequency domain calculation is 4 times shorter than in the time domain calculation, and also the number of time steps needed for the calculation is smaller.

The results of modal analysis were used to set sources for noise propagation problem in the inlet. The method of calculation and the geometry of the computational domain are completely equivalent to those described in the paper [5]. For the calculation of noise propagations we used linearized Euler equations for circumferential modes in the frequency domain, specified on the longitudinal section of the inlet [8]. As a result the flow fields for each of the modes, presented in fig. 4 in the near field of the inlet were obtained.

To compute tone noise radiation in the far field Ffowcs Williams and Hawkings method was used. Finally pressure pulsations were calculated in the points placed along the arc with radius equal to 4 m with the center in the point of intersection between the surface, containing tips of the leading edges of fan rotor blades, and the axis of shaft rotation. The points had uniform angular distribution within 1-90 degrees with 1 degrees spacing.

5. THE COMPARISON WITH EXPERIMENTAL DATA

The results of calculations were compared with the results of the experiment for the fan model in the CIAM test rig C-3A. Comparison was performed for 12 microphones placed at the same distance from the fan, as in the computation. As an initial data for comparison we used narrowband spectra for these microphones obtained in the experiment. The frequency bands of the spectra were equal to 19.5 Hz. On the basis of these spectra the directivity diagrams for the harmonics of tone noise under consideration were calculated.

The results of comparison are presented in the fig. 5. In the figure the directivity diagrams for both the time domain and the frequency domain calculations and the experimental data for frequencies f_2-f_1, f_2, f_2+f_1 and f_2+2f_1 are shown. In general we see good correspondence between the calculations and between them and the experiment.

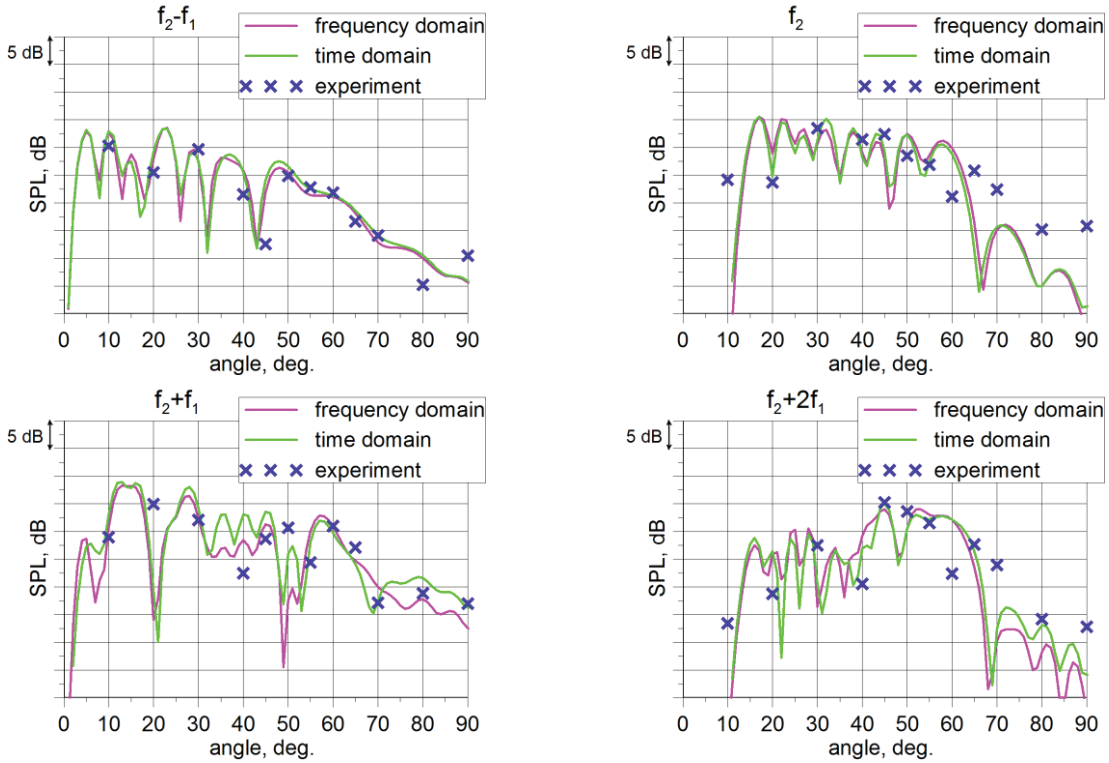

Figure 5. – Comparison between computational and experimental directivity diagrams in a forward hemisphere

6. CONCLUSIONS

The results of the numerical investigation of the first booster stage tone noise at approach

operational conditions are presented. The investigation was performed using the time domain method of calculation, based on multirate Runge-Kutta scheme. The method was developed in CIAM and implemented in CIAM 3DAS solver. The results were compared with the results of the frequency domain calculations of the tone noise of the stage and also with the experimental data obtained in the CIAM C-3A acoustic test facility.

In general the results of the calculations in the time and in the frequency domains are close to each other. Both the powers of different circumferential modes in the inlet and the directivity diagrams in the far field are similar. Especially close results are observed for the directivity diagrams corresponding to the blade passing frequency of the first stage rotor. Also for both calculations there is satisfactory correspondence with experiment. The results can be treated as a strong argument for the validity of the frequency domain method of the multistage turbomachinery tone noise calculations which was presented in our previous works.

REFERENCES

1. N.K. Agarwal, U.W. Ganz, J.W. Premo. – Compressor Noise Contribution To Inlet Noise, AIAA 2004-2913, Proceedings of 10th AIAA/CEAS Aeroacoustics Conference, Manchester, UK, May10–12, 2004
2. Broszat D., Korte D., Tapken U., Moser M. – Validation of turbine noise prediction tools with acoustic rig measurements, AIAA 2009-3283, Proceedings of 15th AIAA/CEAS Aeroacoustics Conference , Miami, Florida, 11 - 13 May 2009
3. D. Korte, T. Hüttl, F. Kennepohl, K. Heinig – Numerical simulation of multistage turbine sound generation and propagation, Aerospace Science and Technology, v. 9, pp. 125–134, 2005
4. Pinelli, L., Poli, F., Marconcini, M., Arnone, A., Spano, E., and Torzo, D. – Validation of a d linearized method for turbomachinery tone noise analysis, GT2011-45886, ASME Turbo Expo 2011, Vancouver, British Columbia, Canada, June 6-10, 2011
5. Rossikhin A.A., Pankov S.V., Mileshin V.I., – Numerical Investigation of The First Booster Stage Tone Noise of a High Bypass Ratio Turbofan, GT2016-57352, ASME Turbo Expo 2016, Seoul, South Korea, June 13-17, 2016.
6. Verdon, J.M. – Linearized Unsteady Aerodynamic Analysis of the Acoustic Response to Wake/Blade-Row Interaction, NASA/CR—2001-210713, 2001.
7. Nyukhtikiv M., Brailko I., Mileshin V., Pankov S. – Computational and Experimental Investigation of Unsteady and Acoustic Characteristics of Counter – Rotating Fans, HT-FED2004-56435, Proceedings of 2004 ASME Heat Transfer / Fluids engineering Summer Conference, Charlotte, North Carolina USA, July 11-15, 2004.
8. Nyukhtikov, M.A., Rossikhin, A.A., Sgadlev, V.V., Brailko, I.A. – Numerical Method for Turbo-Machinery Tonal Noise Generation and Radiation Simulation Using CAA Approach, GT2008-51182, ASME Turbo Expo 2008: Power for Land, Sea and Air, GT2008, Berlin, Germany, June 9-13, 2008
9. Tam C.K.W., Webb J.C. – Dispersion-Relation-Preserving Schemes for Computational Acoustics, Journal of Computational Physics, Vol. 107, pp. 262-281, 1993.
10. Hu F.Q., Hussaini M.Y., Manthey J. – Low-Dissipation and Low-Dispersion Runge-Kutta Schemes for Computational Acoustics, Journal of Computational Physics, Vol. 124, pp. 177-191, 1996
11. Rossikhin A.A., Druzhinin I.M, Khaletskii I.D. Mileshin V.I., – Numerical and Experimental Investigation of Acoustic Characteristics of Model Ultra High Bypass Ratio Counter-Rotating Fan, GT2018-76878, ASME Turbo Expo 2018, Oslo, Norway, June 11-15, 2018.
12. Kvaeligrno A, Rentrop P., Low Order Multirate Runge-Kutta Methods in Electric Circuit Simulation, 1999
13. Hairer E., Norsett S.P., and Wanner G. Solving ordinary differential equations I, Nonstiff problems. Springer-Verlag, second edition, 1993.
14. Khaletskiy Y., Mileshin V. – Experimental Study Of 700-mm Fan Model Noise At CIAM Anechoic Chamber, GT2013-94454, ASME Turbo Expo 2013, San Antonio, Texas, USA, June 3-7, 2013.
15. Rossikhin A.A., Pankov S.V., Mileshin V.I., – Numerical and Experimental Investigation of the First Booster Stage Tone Noise at Different Operational Conditions, ISUAAAT15-057, Proceedings of the 15th International Symposium on Unsteady Aerodynamics, Aeroacoustics & Aeroelasticity of Turbomachines, 24-27 September 2018, University of Oxford, UK